

Ultra high-density silicon nanowires for extremely low reflection in visible regime

Ting-Hang Pei, Subramani Thiyagu, and Zingway Pei

Citation: [Applied Physics Letters](#) **99**, 153108 (2011); doi: 10.1063/1.3650266

View online: <http://dx.doi.org/10.1063/1.3650266>

View Table of Contents: <http://scitation.aip.org/content/aip/journal/apl/99/15?ver=pdfcov>

Published by the [AIP Publishing](#)

Articles you may be interested in

[Porous silicon formation during Au-catalyzed etching](#)

J. Appl. Phys. **115**, 164308 (2014); 10.1063/1.4873892

[High-pressure polyol synthesis of ultrathin silver nanowires: Electrical and optical properties](#)

APL Mat. **1**, 042118 (2013); 10.1063/1.4826154

[Competition between uncatalyzed and catalyzed growth during the plasma synthesis of Si nanowires and its role on their optical properties](#)

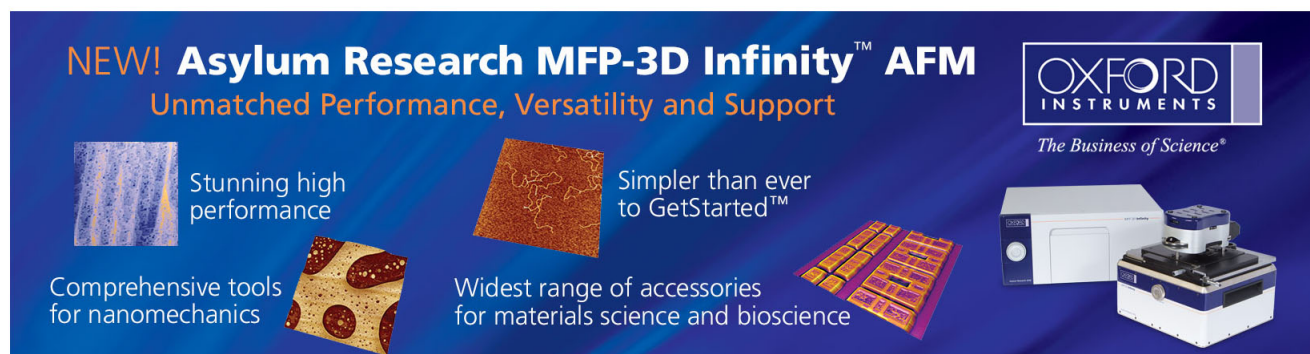
J. Appl. Phys. **113**, 214313 (2013); 10.1063/1.4809557

[Optical properties of "black silicon" formed by catalytic etching of Au/Si\(100\) wafers](#)

J. Appl. Phys. **113**, 173502 (2013); 10.1063/1.4803152

[Influence of catalytic gold and silver metal nanoparticles on structural, optical, and vibrational properties of silicon nanowires synthesized by metal-assisted chemical etching](#)

J. Appl. Phys. **112**, 073509 (2012); 10.1063/1.4757009

The advertisement features a dark blue background with white and orange text. At the top left, it reads 'NEW! Asylum Research MFP-3D Infinity™ AFM' in large white letters, followed by 'Unmatched Performance, Versatility and Support' in orange. On the right, the Oxford Instruments logo is shown with the tagline 'The Business of Science®'. Below the text are four images: a blue textured surface, a brown textured surface, a grid of colorful squares, and a photograph of the AFM instrument. Each image is accompanied by a short text description: 'Stunning high performance', 'Simpler than ever to GetStarted™', 'Comprehensive tools for nanomechanics', and 'Widest range of accessories for materials science and bioscience'.

Ultra high-density silicon nanowires for extremely low reflection in visible regime

Ting-Hang Pei,¹ Subramani Thiyagu,² and Zingway Pei^{2,a)}

¹Microelectronics and Information Systems Research Center, National Chiao Tung University, HsinChu 300, Taiwan

²Graduate Institute of Optoelectronic Engineering, Department of Electrical Engineering, National Chung Hsing University, Taichung 40227, Taiwan

(Received 12 January 2011; accepted 19 September 2011; published online 12 October 2011)

We fabricated large-area, vertically aligned silicon nanowire (SiNW) arrays on Si substrates employing catalytic etching on a polystyrene nanosphere template. The density of SiNWs was as high as $10^{10}/\text{cm}^2$, and the bottom radii of SiNWs ranged between 30 and 60 nm. The reflection from the SiNW layer was approximately 0.1% over the spectral range of 300–800 nm for SiNWs longer than 750 nm. Effective medium theory was applied to explain this extremely low reflection, and it was confirmed that the incident light scatters randomly inside cone-like SiNWs, which lengthens the actual traveling path of light. © 2011 American Institute of Physics. [doi:10.1063/1.3650266]

Surface sub-wavelength structures (SWSs) have attracted research interest because of their remarkable antireflection behavior.^{1–4} Such antireflection surfaces (ARSs) can enhance light transmission and are an industrially important optical element for contemporary optoelectronics.^{5,6} For instance, an ARS enhances the performance of a solar cell by increasing light coupling⁷ and increases backlight transmission and decreases ghosting in flat-panel displays.⁸ To achieve low reflection, SWSs comprise small protrusion arrays with spacing smaller than the wavelength of incident light. This structure, called a zero-order grating,⁹ exists in biological systems, such as the eye of a moth.

Si nanowires (SiNWs) with sub-wavelength structure were recently proposed for solar cells because of their efficient light-harvesting property, which increases the photocurrent.^{5,10–12} The strong light-trapping effect of long SiNWs increases the effective path travelled by light inside SiNWs by a factor of up to 73 as compared with film of the same thickness. However, the SWS is generally produced by lithography as a periodic structure, and the reflection property of an aperiodic SiNW array has rarely been reported.

In this study, we investigated large-scale, high-density ($\sim 10^{10}/\text{cm}^2$), and high-aspect-ratio aperiodic SiNWs fabricated using a polystyrene (PS) nanosphere template (30–60 nm in diameter). The reflectance of the SiNWs was approximately 0.1% over the spectral range of 300–800 nm. The effective medium theory (EMT)^{13–15} and TMM (Ref. 16) were used to explain the extremely low reflection.

PS nanospheres, obtained by using a modified block-copolymer nano-patterning method, were used as templates for SiNW fabrication. The details have been published elsewhere.¹⁷

SiNW was produced via silver (Ag) catalyst chemical etching.¹⁸ Figure 1 is cross-sectional scanning electron microscopy (SEM) images of SiNWs fabricated with chemical etching durations of 90 s. The corresponding SiNW length is approximately 1150 nm. The lengths of SiNWs can be controlled by the duration of the catalyst etching. The bottom

radius of each SiNW was approximately 60 nm. The reflectance spectra of SiNWs for normally incident light were recorded from 300 to 800 nm. Ultra-low reflectance of about 0.1% was achieved when the SiNW was longer than 750 nm. All reflectance measurements, together with calculation results, are shown in Fig. 3. To explain the extremely low reflection, the normal reflectance of SiNWs was calculated theoretically.

Stavenga *et al.*¹⁴ explained the optical properties of a moth's eye-like structure by considering three categories of structural shape: cone, paraboloid, and Gaussian shapes. According to SEM images, the SiNWs in this work could be described as being paraboloids or cones with a bottom radius of r , as shown in Fig. 2. EMT is used to calculate the reflection of SiNWs in a normally incident situation. EMT appropriately describes the optical performance of the SiNWs since the variance of the dielectric constant is small in the considered wavelength regime.^{19–23} According to EMT, one-dimensional quasi-periodic structures are birefringent, and the effective refraction index of two-dimensional structures is independent of polarization.^{24,25}

The reflectance of the SiNW layer is calculated with a multilayer model, as shown in Fig. 2. A cylindrical

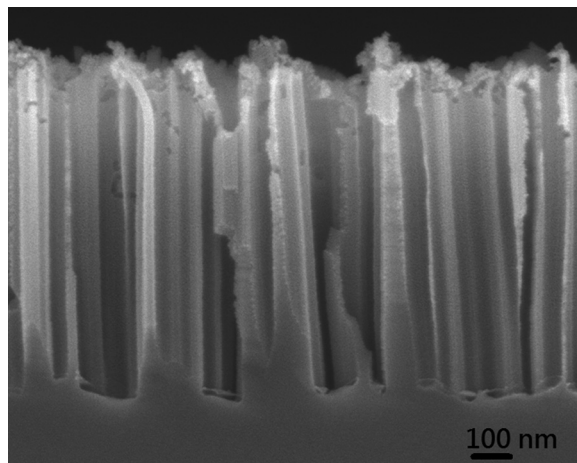


FIG. 1. SEM images of SiNWs with catalyst chemical etching time of 90 s.

^{a)}Electronic mail: zingway@dragon.nchu.edu.tw.

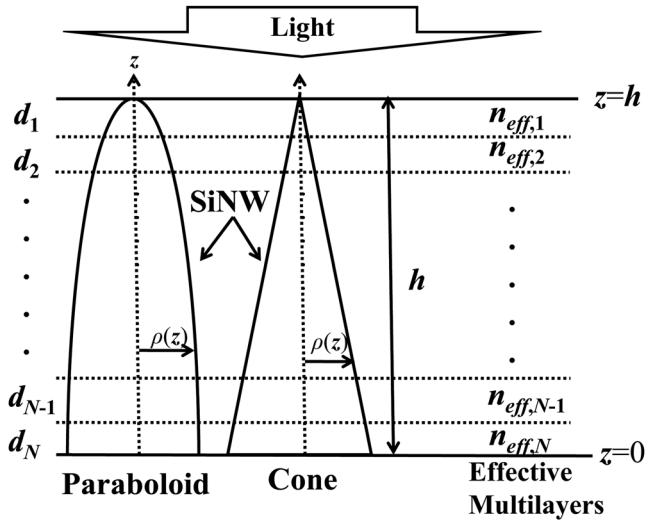


FIG. 2. The paraboloid and cone shapes of SiNWs and effective multilayer structure.

coordinate system is used, in which the z -axis is perpendicular to the substrate surface. The bottom of the SiNW is at $z=0$ and the peak at $z=h$. The SiNW is divided into N horizontal layers with the thickness of each layer denoted d_j , where $j=1, \dots, N$. Each layer has the same thickness, $d_1 = \dots = d_N = d$, in our calculations. The radius of the SiNW, ρ , in each layer satisfies $\rho^2 = (h-z)r^2/h$ and $\rho = (h-z)r/h$ for $0 \leq z \leq h$ for the paraboloid and cone structures, respectively. Therefore, each layer has a different filling ratio $f_j = \pi\rho^2$, resulting in stepwise-varying refraction index profiles. The imaginary part of the refraction index was considered in calculations to match the absorption nature of Si.²⁶

TMM (Ref. 16) was applied to calculate the transmission of electromagnetic waves through the multilayer structure. The incident light was normal to SiNWs, i.e., parallel to the z -axis. Each layer consisted of both forward-traveling and backward-traveling waves. Waves travelling across the interface between two adjacent layers can be described by two dynamic matrices, each written as

$$D_j = \begin{pmatrix} 1 & 1 \\ \eta_j & -\eta_j \end{pmatrix}, \quad (1)$$

where $\eta_j = \sqrt{\varepsilon_j/\mu_j}$. ε_j and μ_j are the relative permittivity and permeability, respectively. We assume that the relative permittivity of each SiNW layer and the Si substrate is equal to 1, the same as for air. The complex effective refraction index $n_{\text{eff},j}$ of layer j is $\sqrt{\varepsilon_j} = n_j - iK_j$, where n_j is the real part of the refraction index and K_j is the extinction coefficient. The imaginary part relates to the absorption of the medium. Each layer in the multilayer structure has a propagation matrix

$$P_j = \begin{pmatrix} e^{i\phi_{j+}} & 0 \\ 0 & e^{-i\phi_{j-}} \end{pmatrix}, \quad (2)$$

Here $\phi_{j+} = n_{\text{eff},j}(\omega d_j/c) = (n_j - iK_j)(\omega d_j/c)$ and $\phi_{j-} = n_{\text{eff},j}(\omega d_j/c) = (n_j + iK_j)(\omega d_j/c)$ are the propagation phases of the forward-traveling and backward-traveling waves,

respectively. ω and c are the frequency and speed of the incident light in a vacuum, respectively. Thus, the propagation waves decay when propagating through the absorption medium. The overall transmission matrix M is written as

$$M = \begin{pmatrix} M_{11} & M_{12} \\ M_{21} & M_{22} \end{pmatrix} = D_{\text{air}}^{-1} \left[\prod_{j=1}^N D_j P_j D_j^{-1} \right] D_{\text{Si}}, \quad (3)$$

where D_{air} and D_{Si} are the dynamic matrices of air and Si, respectively. Reflectance is then calculated according to $R = |M_{21}/M_{11}|^2$.

The effective refraction index varying with the wavelength of light can be approximated as¹⁹

$$n_{\text{eff},j} = \sqrt{f_j n_{\text{Si}}^2 + (1-f_j)n_{\text{air}}^2 + \frac{\pi^2}{3} \left(\frac{a}{\lambda}\right)^2 f_j^2 (1-f_j^2)^2 (n_{\text{Si}}^2 - n_{\text{air}}^2)}, \quad (4)$$

where a is the periodicity, λ is the wavelength of light, and n_{air} and n_{Si} are the refraction indices of air and Si, respectively. This approximation is referred to as second-order EMT for convenience. The thickness of each layer, d , is chosen as 1 nm in all calculations. The numerical errors are believed to be less than 1%. Four different lengths of SiNWs, 280, 750, 1150, and 1500 nm, are considered. Two SiNW shapes, the cone and paraboloid, are used for each length. In our simulation model, each SiNW is supposed to be located in a square, and the position of the SiNW is randomly distributed within the square. Each square is close to its neighbors. If the bottom radius r of the SiNW equals the half-length of the square, the paraboloids or cones are in contact with each other. Since almost all SiNWs connect with neighbors at their base as shown in Fig. 1, the bottom radius r is chosen reasonably as $0.5a$ in all simulations, where a is the periodicity of the square. Additionally, the SiNWs have different radii in the range of 30–60 nm. Therefore, the periodicity is chosen from 60 to 120 nm in simulations. Finally, we take the average reflectance as the calculation results.

The reflectance in the experiment and calculation results for four SiNW lengths are presented in Figs. 3(a)–3(d). The experimentally determined reflectance of SiNWs in the range from 300 to 800 nm tends to decrease as the length increases. The reflectance calculated with the second-order EMT of a paraboloid shape is greater than the experimental reflectance. In contrast, the reflectance based on a cone-shaped SiNW more favorably fits the experimental results except at wavelengths less than 380 nm. The EMT model predicts that the reflectance increases rapidly at wavelengths less than 380 nm. However, the reflectance measured at wavelengths less than 380 nm is still quite low. This might be due to first-order diffraction that couples light strongly to the SiNW and reduces reflectance in reality. The reflectance spectra calculated at wavelengths longer than 380 nm indicate that the shape of SiNWs in our experiment is more appropriately described as a cone. However, the calculation results do not fit the experimental data well. Interference was clearly observed in the calculation reflectance, whereas the experimental reflectance shows no interference. This might relate to the fabrication of SiNWs, where chemical etching

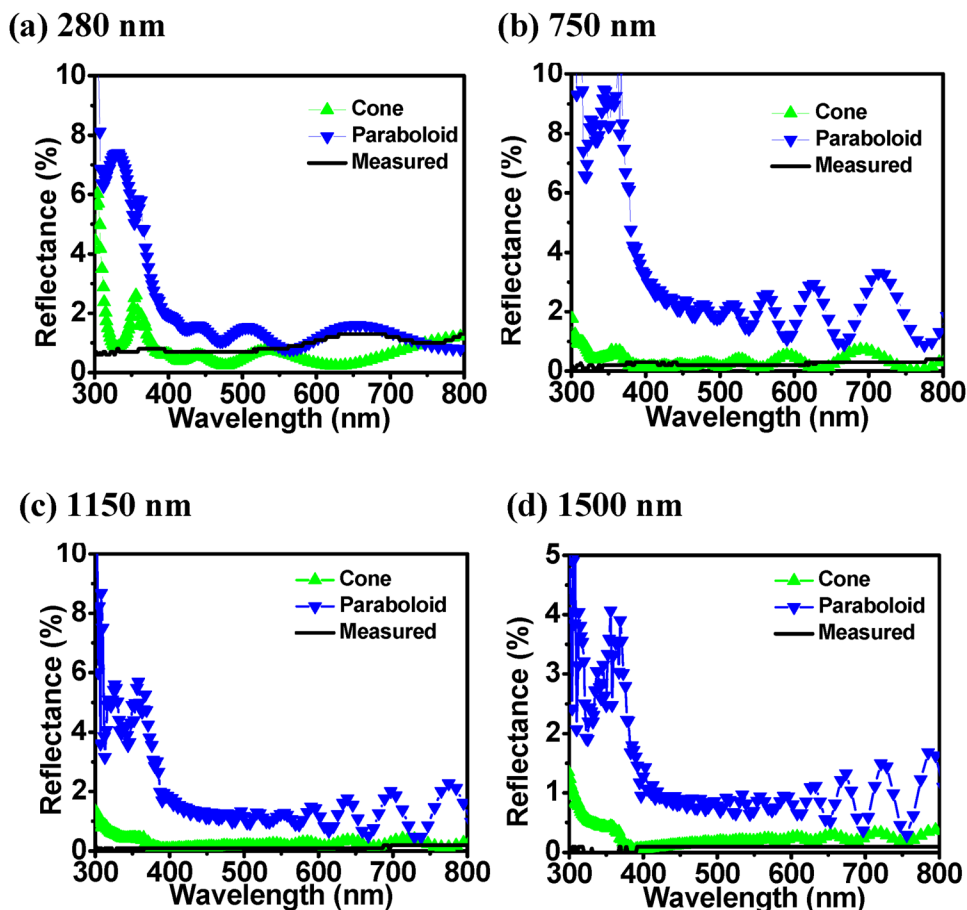


FIG. 3. (Color online) Reflectance spectra of experimental data and the second-order EMT combined with paraboloid and cone shapes for SiNW height (a) 280, (b) 750, (c) 1150, and (d) 1500 nm, respectively.

produces a rough SiNW surface. In other words, each SiNW has different length and deviates the average in a certain range. So each experimental reflectance in Fig. 3 appears to be the average reflectance, and the constructive interference disappears due to the rough surface and randomly distributed SiNWs.

In summary, we fabricated high-density and high-aspect-ratio SiNWs exhibiting extremely low reflectance over a wavelength range from 300 to 800 nm employing silver catalyst chemical etching on a PS nanosphere template. The length of SiNWs can be controlled by the etching duration. As the length of SiNWs exceeds 750 nm, the reflectance is as low as 0.1% at wavelengths from 300 to 800 nm. A model based on cone-shaped Si nanowires was used to calculate the reflectance employing the second EMT method. The calculated reflectance fits the measured reflectance better for long SiNWs at wavelengths longer than 380 nm.

This work is supported by National Science Council of Taiwan, R.O.C. under Grant NSC-98-ET-E-005-003-ET.

¹Y. Kanamori, M. Sasaki, and K. Hane, *Opt. Lett.* **24**, 20, 1422 (1999).

²C.-H. Sun, P. Jiang, and B. Jiang, *Appl. Phys. Lett.* **92**, 061112 (2008).

³Y. Kanamori, K. Hane, H. Sai, and H. Yugami, *Appl. Phys. Lett.* **78**, 142 (2001).

⁴Y. F. Li, J. H. Zhang, S. J. Zhu, H. P. Dong, F. Jia, Z. H. Wang, Z. Q. Sun, L. Zhang, Y. Li, H. B. Li, W. Q. Xu, and B. Yang, *Adv. Mater.* **21**, 4731 (2009).

⁵J. H. Li, H. Y. Yu, S. M. Wong, G. Zhang, X. W. Sun, P. G.-Q. Lo, and D.-L. Kwong, *Appl. Phys. Lett.* **95**, 033102 (2009).

⁶T. Hoshino, M. Itoh, and T. Yatagai, *Appl. Opt.* **46**, 648 (2007).

⁷*Handbook of Photovoltaic Science and Engineering*, edited by A. Luque and S. Hegedus (Wiley, West Sussex, 2003).

⁸J. A. Hiller, J. D. Mendelsohn, and M. F. Rubner, *Nat. Mater.* **1**, 59 (2002).

⁹S. J. Wilson and M. C. Hutley, *Opt. Acta* **29**, 993 (1982).

¹⁰L. Hu and G. Chen, *Nano Lett.* **7**, 3249 (2007).

¹¹V. Sivakov, G. Andrä, A. Gawlik, A. Berger, J. Plentz, F. Falk, and S. H. Christiansen, *Nano Lett.* **9**, 1549 (2009).

¹²E. Garnett and P. D. Yang, *Nano Lett.* **10**, 1082 (2010).

¹³D. H. Raguin and G. M. Morris, *Appl. Opt.* **32**, 1154 (1993).

¹⁴D. G. Stavenga, S. Foletti, G. Palasantzas, and K. Arikawa, *Proc. R. Soc. London, Ser. B* **273**, 661 (2006).

¹⁵P. Y. Han, Y. T. W. Chen, and X.-C. Zhang, *IEEE J. Sel. Top. Quantum Electron* **16**, 338 (2010).

¹⁶P. Yeh, *Optical Waves in Layered Media* (Wiley, Singapore, 1991).

¹⁷S. Thiyagu, Z. Pei, M. W. Ho, S. J. Cheng, W. S. Hsieh, and Y. Y. Lin, *Nanosci. Nanotechnol. Lett.* **3**, 215 (2011).

¹⁸Z. Huang, H. Fang, and J. Zhu, *Adv. Mater.* **19**, 744 (2007).

¹⁹D. E. Aspnes, *Am. J. Phys.* **50**, 704 (1982).

²⁰R. C. Tyan, P. C. Sun, A. Scherer, and Yeshayahu, *Opt. Lett.* **21**, 761 (1996).

²¹J.-S. Chen, S. Chao, J.-S. Kao, H. Niu, and C.-H. Chen, *Appl. Opt.* **35**, 90 (1996).

²²L. Ward, *The Optical Constants of Bulk Materials and Films* (IOP Publishing Ltd., England, 1998), Chap. 8.

²³S. Sinzinger and J. Jahns, *Microoptics* (Wiley-VCH, New York, 1999).

²⁴W. Stork, N. Streibl, H. Haidner, and P. Kipfer, *Opt. Lett.* **16**, 1921 (1991).

²⁵Y. Kanamori, M. Sasaki, and K. Hane, *Opt. Lett.* **24**, 1422 (1999).

²⁶E. D. Palik, *Handbook of Optical Constants of Solids* (Academic, San Diego, 1998), Vol. 1.